Available online at www.sciencedirect.com
SCIENCE DIRECT®
Journal of Crystal Growth 287 (2006) 591–595
JOURNAL OF CRYSTAL GROWTH
www.elsevier.com/locate/jcrysgro

Correlation of the structural and ferromagnetic properties of $Ga_{1-x}Mn_xN$ grown by metalorganic chemical vapor deposition

Matthew H. Kane[a,b], Martin Strassburg[a], William E. Fenwick[a], Ali Asghar[a], Adam M. Payne[a], Shalini Gupta[a], Qing Song[c], Z. John Zhang[b], Nikolaus Dietz[d], Christopher J. Summers[a], Ian T. Ferguson[a,b,*]

[a]*School of Electrical and Computer Engineering, Georgia Institute of Technology, Atlanta, GA 30332, USA*
[b]*School of Materials Science and Engineering, Georgia Institute of Technology, Atlanta, GA 30332, USA*
[c]*School of Chemistry and Biochemistry, Georgia Institute of Technology, Atlanta, GA 30332, USA*
[d]*Department of Physics and Astronomy, Georgia State University, Atlanta, GA 30303, USA*

Available online 5 December 2005

Abstract

Metalorganic chemical vapor deposition (MOCVD) has been used to grow high-quality epitaxial films of $Ga_{1-x}Mn_xN$ of varying thickness and manganese doping levels. No macroscopic second phases were observed via high resolution X-ray diffraction. Atomic force microscopy revealed MOCVD-like step flow growth patterns with a mean surface roughness as low as 3.78 Å in lightly doped samples, and matched that of the underlying GaN template layers. No change in the growth mechanism and morphology with Mn incorporation is observed. A uniform Mn concentration in the epitaxial layers is confirmed by secondary ion mass spectrometry. SQUID measurements showed an apparent RT ferromagnetic hysteresis with saturation magnetizations as high as $2.4\mu_B$/Mn at $x = 0.008$, which decreases with increasing Mn incorporation or reduced structural quality. Co-doping with either Si or Mg during the resulting growth process resulted in a large decrease in the saturation magnetization values. Competition for incorporation between Mn and Mg during the MOCVD growth process is observed.

PACS: 75.50.Pp; 75.50.Ak; 78.55.Cr; 81.05.Ea; 81.15.Gh; 81.05.Zx; 85.75.−d

Keywords: A3. Metalorganic chemical vapor deposition; B2. Magnetic materials; B2. Semiconducting gallium compounds

1. Introduction

Nitride-based ferromagnetic (FM) semiconductors have been the subject of interest for the past half-decade for potential applications within the field of spintronics, which seeks to exploit both the spin and charge of an electron for improved or novel device functionalities [1]. For practical applications, materials which are both compatible with traditional semiconductor electronics and can support the storage and/or transport of spins at room temperature (RT) are required. The latter stipulation demands that the Curie temperature of the material used be greater than RT, which is problematic in the well-established III–V diluted magnetic semiconductors (DMS) such as $Ga_{1-x}Mn_xAs$ which have Curie temperatures well less than 200 K.

Using the fundamental assumptions that FM in the III–V semiconductors is mediated by the charge carriers within the system, theoretical predictions have suggested that this may be able to be pushed above RT in wide band gap DMS [2]. Curie temperatures up to 940 K have been reported in $Ga_{1-x}Mn_xN$ [3] in materials produced by a number of different growth techniques including ion implantation [4], molecular beam epitaxy (MBE) [5], and metalorganic chemical vapor deposition (MOCVD) [6]. In contrast to the production of $Ga_{1-x}Mn_xAs$, growth has been at temperatures approaching the normal GaN growth temperatures. For the nitrides, there is a trade-off between

*Corresponding author. School of Electrical and Computer Engineering, Georgia Institute of Technology, Atlanta, GA 30332-0250, USA. Tel.: +1 404 385 2885; fax: +1 404 385 2886.
E-mail address: ianf@ece.gatech.edu (I.T. Ferguson).

0022-0248/$ - see front matter © 2005 Elsevier B.V. All rights reserved.
doi:10.1016/j.jcrysgro.2005.10.081

preventing the formation of magnetic second phases during the growth and production of material that is of sufficient quality for doping and device applications.

This observation is problematic in light of a more thorough analysis of the prevailing theories for FM in DMS. There are numerous reports of RT FM which do not meet the original criteria for Mn and hole concentration of 5% and 10^{20} holes/cm^3, respectively. This has led to alternate suggestions of the FM origin observed in these samples, including FM Mn-rich second-phase precipitation [7], artifacts of the magnetization measurement process [8], or clusters of Mn within the semiconductor lattice [9]. Other theories suggest FM may still be possible, although there is some controversy about the anticipated Curie temperature. In the nitrides, Mn is a well-established deep trap, and thus the d-states should be highly localized within the band gap [10]. Double exchange d–d exchange interactions have been suggested as an alternate mechanism of FM [11], though this interaction is short-ranged and should not lead to RT FM in the dilute limit [12]. Another theory suggests that FM is stabilized within a spin-split impurity band which may be related to extended defects in the wide band gap DMS [13]. Recent observations suggest that the FM observed in the related material $Ga_{1-x}Mn_xP$ [14] is concomitant with a detached but shallow impurity band [15].

In order to determine the origins of FM in the nitrides and develop these materials for spintronic devices, it is crucial to understand how the non-equilibrium crystal growth techniques affect the Mn distribution, structural properties and resulting electrical and magnetic properties of the material. The role of defects will be particularly important, as compensation effects may play a crucial role in the electrical and magnetic behavior. This paper investigates these effects during the MOCVD growth of $Ga_{1-x}Mn_xN$.

2. Experimental procedure

In this work, $Ga_{1-x}Mn_xN$ films were grown in a highly modified commercial rotating-disk reactor with a short jar configuration. A specially designed reactant injection system with dual injector blocks is used to minimize pre-reactions of the gallium and manganese precursors in the transport phase. Mn concentrations up to ~2% were obtained in the epilayers by controlling the molar flow ratios of the precursors. All films were grown on 2″ sapphire (0 0 0 1) substrates, indicating the scalability of this for potential future device applications. Initially, GaN buffer layer templates with a thickness of 1–2 μm were grown, followed by $Ga_{1-x}Mn_xN$ at temperatures of 900 and 1050 °C of varying thicknesses ranging from 300 to 1000 nm. Some films were grown without these template layers, using low Mn doping levels within the buffer layer. Some samples were subsequently annealed face-down on GaN templates in a flowing nitrogen ambient at temperatures ranging from 700 to 900 °C. Ammonia, trimethyl gallium (TMG), trimethyl aluminum (TMA) and bis-cyclopentadienyl manganese (Cp_2Mn), bis-cyclopentadienyl magnesium (Cp_2Mg) and silane (SiH_4) were used as the nitrogen, metal and dopant sources. A subsequent characterization performed included high-resolution X-ray diffraction (Philips X'Pert Pro diffractometer) secondary ion mass spectrometry (SIMS) (Atomika Instruments Ionmicroprobe A-DIDA 3000), atomic force microscopy (AFM) (PSIA XE-100), and low- and high-temperature magnetometry (Quantum Design MPMS 5S SQUID magnetometer and Lakeshore 7404 Vibrating Sample Magnetometer).

3. Results and discussion

The as-grown films are specular and have a reddish color which depends on the doping level of the Mn, as well as the thickness of the Mn-containing layers. High resolution X-ray diffraction scans perpendicular to the substrate plane revealed only the basal plane reflections of GaN and the sapphire substrate, as would be expected for an epitaxial film. In optimally grown samples at less than 2% Mn incorporation, no second phases are visible. However, with increasing annealing, second phases do appear in the X-ray diffraction scans and most closely index to the antiferromagnetic phase $GaMn_3N$, most likely on the surface. X-ray diffraction line widths of the $\omega-2\theta$ scans are approximately 170 arcsec for the (0 0 2) reflection and 500 arcsec for the (1 0 2) reflections under the optimal growth conditions. The addition of Si or Mg to the growth process did not change the line widths of the symmetric reflections significantly. The lattice parameter of the thin films could not be distinguished from that of the underlying template layer, even for films grown using Mn in the buffer layer and no GaN template layer.

AFM was used to investigate the surface morphology of the as-grown samples. Fig. 1 shows AFM images for samples grown at temperatures within and below the optimum growth temperature window. In the first image of a typical Mn-doped layer, clear step-flow atomic growth steps typical of standard two-dimensional MOCVD growth are seen. There appears to be no change of the growth mode with small Mn alloying concentration during the growth. The surface roughness varied from sample to sample, between 3 and 11 Å in the Mn doped samples, though this is almost entirely dependent on the roughness of the GaN template layer. If the temperature is varied low outside the normal growth window, the surface morphology roughens considerably, and hexagonal type temperature defect facets are clearly evident due to the lower surface diffusion rates of the adatoms. Upon high-temperature annealing in a non-reactive environment, the surface roughens and there is some clustering or phase decomposition occurring at the surface. This is coincident with a decrease in the observed magnetization signal, as is the case with samples grown at lower temperatures.

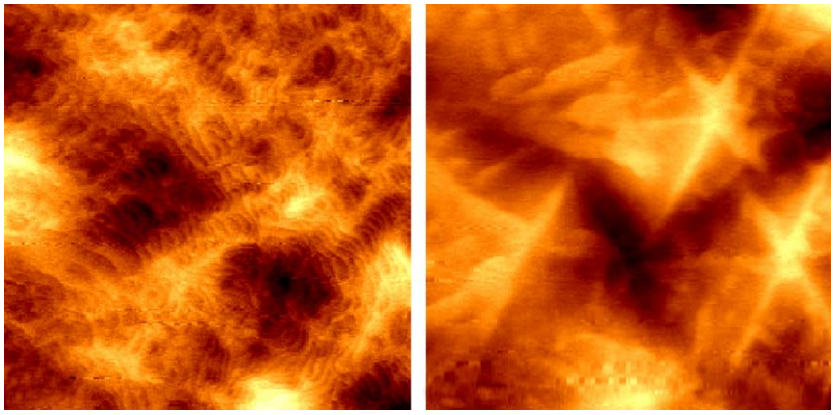

Fig. 1. Atomic force microscopy of $Ga_{1-x}Mn_xN$ grown by MOCVD at high (left) and low (right) temperatures. Both images are $10 \times 10\,\mu m^2$. RMS roughnesses are 5.6 and 14.1 Å, respectively.

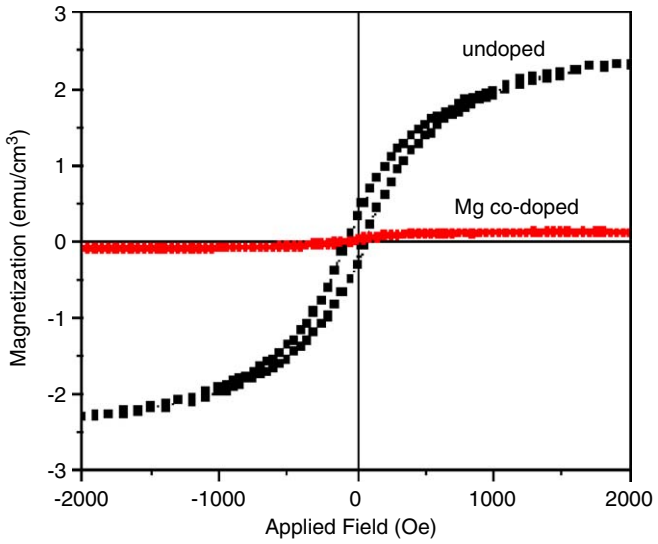

Fig. 2. Measured RT VSM curves for $Ga_{1-x}Mn_xN$ with and without Mg co-doping. The linear background of the sample holder and substrate have been subtracted.

Superconducting quantum interference device (SQUID) and vibrating sample (VSM) magnetometry were performed to determine the macroscopic magnetic properties of the MOCVD-grown $Ga_{1-x}Mn_xN$ films. FM hysteresis was recorded in the as-grown $Ga_{1-x}Mn_xN$ films. Fig. 2 shows representative magnetization behavior of these samples. There is little deviation for the hysteresis curves at 300 and 5 K, indicating that the hysteresis is likely due to a phase with a high Curie temperature ($T_C > 400$ K). The highest saturation magnetization of the as-grown $Ga_{1-x}Mn_xN$ samples with $x = 0.008$ is 11.6 emu/cm^3 which, based on the expected doping levels associated with the precursor molar flows, corresponds to a magnetic moment of $2.4\mu_B$/Mn. A weaker FM signature per Mn is observed with increasing doping, and some non-optimally grown samples have magnetization values that are an order of magnitude weaker, likely due to electronic compensation effects. The coercivity of the films is between 40–70 Oe in all cases. When the MOCVD-grown samples are co-doped with silicon, a significant drop in the magnetization of the samples occurs, and is nearly destroyed with doping concentrations greater than 10^{19}/cm^3 Si. A comparison of the zero field- and field-cooled magnetization versus temperature curves as a function of Si co-doping are shown in Fig. 3. Two observations are readily apparent: with increasing Si doping, the saturation magnetization of the samples drops considerably. Secondly, that at intermediate doping levels, there is a large splitting in the zero field-cooled and field-cooled temperature-dependent magnetization curves. This leads to the observation of weak or non-existent hysteresis in SQUID M vs. H curves at 5 K if not cooled under an applied field, while those at RT show much more pronounced magnetization. The origin of this observed paramagnetic behavior in the more strongly Si-doped samples, whether related to a reduced magnetic interaction of magnetic clusters, weakened communication between isolated magnetic centers through electronic transport or an experimental artifact is still under investigation. A decrease is also observed in the magnetic behavior with Mg co-doping, as shown in the VSM data in Fig. 2. In the case of the p-type GaMnN:Mg, almost no hysteresis is observed. Mg introduction requires annealing to activate the acceptors. However, at the elevated temperatures required for activation, strong surface decomposition through the creation of nitrogen vacancies or secondary phases is known to occur [16]. Almost no change in the magnetization is observed after annealing, indicating acceptor activation is not strong enough to overcome self-compensation occurring during the growth process.

The origin of the variation in magnetization strength with varying doping level and p-type and n-type doping is still under debate. One school of thought suggests that this variation is due to the depopulation of an impurity band [17]; the location of this band relative to the conduction and valence bands may be anywhere between 1.4 [18] and 1.8 eV [19] above the valence band. Based on the double exchange model, an increase in the hole concentration is

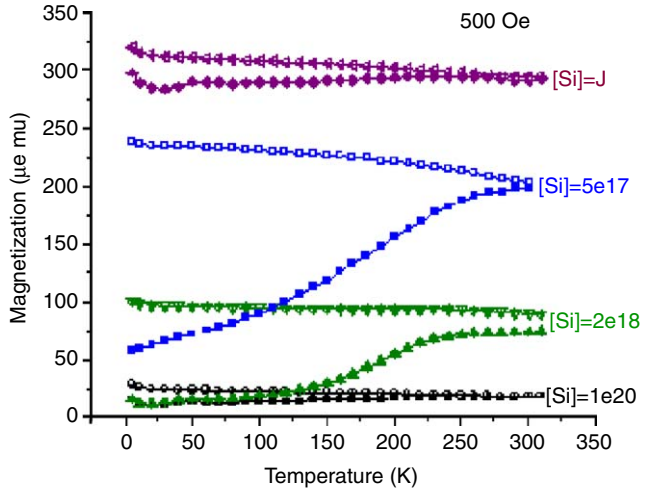

Fig. 3. Field-cooled (upper) and zero field-cooled (lower) magnetization curves for $Ga_{1-x}Mn_xN$ with various silicon co-doping levels.

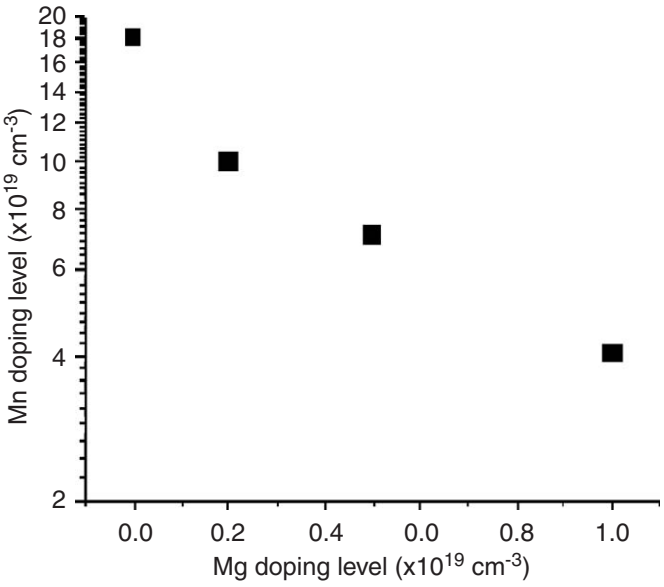

Fig. 4. Mn incorporation as a function of increasing Mg level in MOCVD-grown $Ga_{1-x}Mn_xN$.

predicted to lead to an increase in the Curie temperature and magnetization [20], as should light p-type doping in the cases of an impurity band. This is clearly not the case in these films, and may be a result of overcompensation and structure degradation at the high doping level in the growth process. Another suggestion regarding the effects of the various dopants is that they cause Fermi level-dependent changes in the diffusion of the material [21]. This would foster different diffusion rates in the material and result in enhanced clustering and/or FM second phase formation. Diffusion studies performed on the materials in this study are as yet inconclusive on the differences in Mn diffusion in n-type and undoped GaN via bulk diffusion. An analogous surface diffusion-related effect may be observed on the surface during the growth process, due to anti-surfactant effects. Si is a well-know anti-surfactant in GaN growth and reduces the overall diffusion lengths by providing additional nucleation sites for film growth. Under sufficient flows of silane, the MOCVD growth mode has been reported to shift from a two-dimensional to three-dimensional growth [22]. The large ZFC/FC splittings observed in the magnetization studies may be related to this transition in the growth scheme and reduced Mn cluster size Mn–Mn interactions owing to the Si anti-surfactant effect; this hypothesis is currently under further investigation. Nucleation studies for $Ga_{1-x}Mn_xN$ reported elsewhere in this issue suggest that Mn may also have an anti-surfactant effect [23].

SIMS was used to investigate the effects of growth process and doping on the incorporation of Mn and other elements into the lattice. Compositional and thickness fluctuations are observed over the area of the wafer, due to local variations in the temperature and the flow patterns of the inlet precursor gases. Fig. 4 shows the measured Mn concentration as a function of Mg concentration in the films for a constant flow of Mn gas. The values for the concentrations were calculated using a known ion implantation standard which was measured in parallel to these samples. As the Mg flow rate is increased, there is a large decrease in the Mn concentration. This is not altogether unexpected, as the precursors for Mn and Mg are identical except for the metal within the metalorganic source. The reduced Mn concentration should lead to a corresponding decrease in the overall magnetization, but in this case the magnetization completely disappears. The concentration of Mg is an order of magnitude lower than for the Mn, so it is impossible for this concentration of acceptors to completely depopulate the Mn impurity levels, and should not result in a significant lowering of the Fermi energy, which suggests that the reduced magnetization does not originate from this drifting outside the band on the low side. A similar SIMS profile for the Si co-doped samples does not show the same systematic drop in Mn concentration with increasing n-type doping.

4. Conclusion

$Ga_{1-x}Mn_xN$ films were grown by MOCVD and exhibited similar structural properties and surface morphology to GaN films. A strong magnetic hysteretic signal was observed in some films, and both Mg and Si type co-dopants were found to remove the magnetic behavior. An unusual deviation in the field-cooled and zero field-cooled magnetization spectra was observed with Si co-doping. SIMS measurements indicated that under the growth conditions employed in this study, Mg and Mn are competitive for lattice incorporation in GaN. These results suggest that while there are no macroscopic changes in the MOCVD growth process resulting in the incorporation of Mn, the surface thermodynamics and kinetics during

growth and annealing may play the dominant role in the ultimate behavior of the material.

Acknowledgements

This work has been supported by the National Science Foundation (ECS#0224266, U. Varshney). Support for one author (M.K.) has been provided through a NDSEG fellowship sponsored by the US Department of Defense. M.S. was supported by the Feodor–Lynen program of the Alexander von Humboldt-foundation. The authors thank M. Han for performing additional SQUID measurements; additional vibrating sample magnetometry results were provided by LakeShore Cryonics.

References

[1] S.A. Wolf, D.D. Awschalom, et al., Science 294 (2001) 1488.
[2] T. Dietl, H. Ohno, et al., Science 287 (2000) 1019.
[3] S. Sonoda, S. Shimizu, et al., J. Crystal Growth 237–239 (2002) 1358.
[4] N. Theodoropoulou, A.F. Hebard, et al., Appl. Phys. Lett. 78 (2001) 3475.
[5] M.E. Overberg, C.R. Abernathy, et al., Appl. Phys. Lett. 79 (2001) 1312.
[6] M.H. Kane, A. Asghar, et al., Semicond. Sci. Technol. 20 (2005) L5.
[7] S. Dhar, O. Brandt, et al., Appl. Phys. Lett. 82 (2003) 2077.
[8] R. Giraud, S. Kuroda, et al., Europhys. Lett. 65 (2004) 553.
[9] B.K. Rao, P. Jena, Phys. Rev. Lett. 89 (2002) 185504.
[10] Y.-J. Zhao, P. Mahadevan, et al., Appl. Phys. Lett. 84 (2004) 3753.
[11] K. Sato, H. Katayama-Yoshida, Semicond. Sci. Technol. 17 (2002) 367.
[12] K. Sato, P.H. Dederichs, et al., J. Supercond. 18 (2005) 33.
[13] J.M.D. Coey, M. Venkatesan, et al., Nat. Mater. 4 (2005) 173.
[14] N. Theodoropoulou, A. Hebard, et al., Phys. Rev. Lett. 89 (2002) 107203.
[15] M.A. Scarpulla, B.L. Cardozo, et al., http://arxiv.org/abs/cond-mat/0501275.
[16] M.H. Kane, A. Asghar, et al., MRS Proc. 831 (2005) E9.4.1.
[17] M.J. Reed, F.E. Arkun, et al., Appl. Phys. Lett. 86 (2005) 102504.
[18] L. Kronik, M. Jain, et al., Phys. Rev. B 66 (2002) 041203.
[19] T. Graf, M. Gjukic, et al., Appl. Phys. Lett. 81 (2002) 5159.
[20] H. Katayama-Yoshida, K. Sato, Physica B 327 (2003) 337.
[21] T. Dietl, Phys. Stat. Sol. B 240 (2003) 433.
[22] C. Thompson, G.B. Stephenson, et al., J. Electrochem. Soc. 148 (2001) C390.
[23] S. Gupta, H. Kang, et al., J. Crystal Growth (2005) (in press).